Available online at www.sciencedirect.com
SCIENCE DIRECT
Geochimica et Cosmochimica Acta 70 (2006) 2715–2725
Geochimica
www.elsevier.com/locate/gca

# The long-term fate of $Cu^{2+}$, $Zn^{2+}$, and $Pb^{2+}$ adsorption complexes at the calcite surface: An X-ray absorption spectroscopy study

Evert J. Elzinga *, Ashaki A. Rouff, Richard J. Reeder

*Department of Geosciences, Center for Environmental Molecular Science, Stony Brook University, Stony Brook, NY 11794-2100, USA*

Received 10 August 2005; accepted in revised form 27 February 2006

**Abstract**

In this study, the speciation of $Zn^{2+}$, $Pb^{2+}$, and $Cu^{2+}$ ions sorbed at the calcite surface was monitored during a 2.5-year reaction period, using extended X-ray absorption spectroscopy to characterize metal speciation on the molecular scale. Experiments were performed using pre-equilibrated calcite-water suspensions of pH 8.3, at metal concentrations below the solubility of metal hydroxide and carbonate precipitates, and at constant metal surface loadings. The EXAFS results indicate that all three metals remained coordinated at the calcite surface as inner-sphere adsorption complexes during the 2.5-year ageing period, with no evidence to suggest slow formation of dilute metal-calcite solid solutions under the reaction conditions employed. All three divalent metals were found to form non-octahedral complexes upon coordination to the calcite surface, with $Zn^{2+}$ adsorbing as a tetrahedral complex, $Cu^{2+}$ as a Jahn–Teller distorted octahedral complex, and $Pb^{2+}$ coordinating as a trigonal- or square-pyramidal surface complex. The non-octahedral configurations of these surface complexes may have hindered metal transfer from the calcite surface into the bulk, where $Ca^{2+}$ is in octahedral coordination with respect to first-shell O. The use of pre-equilibrated calcite suspensions, with no net calcite dissolution or precipitation, likely prevented metal incorporation into the lattice as a result of surface recrystallization. The results from this study imply that ageing alone does not increase the stability of $Zn^{2+}$, $Pb^{2+}$, and $Cu^{2+}$ partitioning to calcite if equilibrium with the solution is maintained during reaction; under these conditions, these metals are likely to remain available for exchange even after extended sorption times.


## 1. Introduction

The uptake of trace metals and radionuclides by calcite has been studied in considerable detail, because the ubiquity of calcite in the (sub)surface environment combined with its reactive nature makes this mineral a potentially important sink for contaminants in numerous environmental settings. In general, the uptake of metals by mineral sorbents may proceed via a number of different mechanisms, including adsorption (the coordination of metal ions to the mineral surface), coprecipitation (the incorporation of metal ions into the mineral structure by substituting for lattice atoms) and precipitation (the formation of secondary mineral phases). Several studies have shown that all of these uptake mechanisms may be operative in the sequestration of divalent trace metals by calcite, depending on reaction variables such as metal type and concentration, calcite saturation state, reaction time, and pH (Zachara et al., 1988, 1989, 1991; Paquette and Reeder, 1990, 1995; Stipp et al., 1992; Sturchio et al., 1997; Temmam et al., 2000; Elzinga and Reeder, 2002; Godelitsas et al., 2004; Rouff et al., 2004, 2005, 2006).

In many studies it has been found that the stability of partitioned metals increases with sorption time, as evidenced by a decrease in the rate and extent of metal desorption. This indicates that in certain systems, sorbed metal species may undergo slow transformation into more stable sorption products that are less susceptible to release back into solution. Mechanistically, a number of different processes may be involved in the increase in stability of metal partitioning with time; these include metal incorporation into the mineral lattice during recrystallization of the mineral sorbent (e.g., Ainsworth et al., 1994; Van der Weijden

* Corresponding author. Present address: Swiss Federal Institute of Technology (ETH) Zürich, Institute of Terrestrial Ecology, CH-8092 Zürich, Switzerland.
*E-mail address:* evert.elzinga@env.ethz.ch (E.J. Elzinga).

0016-7037/$ - see front matter © 2006 Elsevier Inc. All rights reserved.
doi:10.1016/j.gca.2006.02.026

et al., 1994, 1997a; Ford et al., 1999; Schosseler et al., 1999), metal incorporation into the lattice by solid-state diffusion from the surface into the mineral bulk (Stipp et al., 1992; Stipp, 1994), stabilization of metal precipitate phases by Ostwald ripening and slow structural transformations (Ford et al., 1999; Scheckel et al., 2000), and rearrangement of surface complexes into a more stable configuration (Arai and Sparks, 2002; Dähn et al., 2003).

A number of studies have addressed the effect of reaction time on the mechanism of divalent metal uptake by calcite. Work by Stipp and co-workers (Stipp et al., 1992; Stipp, 1994, 1998; Hoffmann and Stipp, 2001) indicated that $Cd^{2+}$ and $Zn^{2+}$ may move from the calcite surface into the calcite bulk via defect-enhanced solid-state diffusion on relatively short time scales, whereas $Ni^{2+}$ appeared to undergo no solid-state diffusion, and remained mostly present at the calcite surface even after prolonged reaction times. Schosseler et al. (1999) followed the uptake and speciation of $Cu^{2+}$ as a function of time in calcite and vaterite suspensions using in situ electron paramagnetic resonance (EPR) spectroscopy. In the calcite suspensions, where active dissolution and recrystallization of the calcite surface occurred due to the fact that the solutions used in this study were under-saturated with respect to calcite before reaction with $Cu^{2+}$ was initiated, sorbed $Cu^{2+}$ was found to transform from a square planar or square pyramidal adsorbed surface species into an octahedral Jahn–Teller distorted bulk species during recrystallization, resulting in the formation of a dilute $Cu_xCa_{(1-x)}CO_3$ solid solution. The same change in $Cu^{2+}$ coordination was observed in the vaterite experiments during the transformation of vaterite into calcite. Rouff et al. (2002) used batch sorption and desorption experiments to study the reversibility of $Pb^{2+}$ uptake by calcite as a function of reaction time, and observed that $Pb^{2+}$ sorption remained largely reversible during the 12-day reaction time employed. Davis et al. (1987) and Martin-Garin et al. (2003) observed a slow uptake step of $Cd^{2+}$ on calcite, which was correlated to a decrease in reversibility of $Cd^{2+}$ sorption, and interpreted to be due to solid solution formation (Davis et al., 1987) and solid-state diffusion (Martin-Garin et al., 2003), respectively. Van der Weijden et al. (1994) observed a decrease in reversibility of $Cd^{2+}$ sorption to calcite over time, as determined via desorption experiments, which was attributed to $Cd^{2+}$ incorporation into the calcite lattice during calcite recrystallization associated with steady-state exchange between the solid and liquid phase.

In the present study, we use extended X-ray absorption fine structure spectroscopy (EXAFS) to investigate the effect of reaction time on the speciation of $Zn^{2+}$, $Pb^{2+}$, and $Cu^{2+}$ sorbed at the calcite surface in pre-equilibrated calcite–water suspensions of pH 8.3 at metal concentrations below the solubility of metal hydroxide and carbonate precipitate phases. Recent EXAFS studies have shown that under these conditions $Zn^{2+}$, $Pb^{2+}$, and $Cu^{2+}$ coordinate at the calcite surface as inner-sphere mononuclear adsorption complexes when employing short incubation times on the order of days (Elzinga and Reeder, 2002; Rouff et al., 2004; Lee et al., 2005). The results presented here characterize the speciation of these calcite-sorbed metals during a 2.5-year reaction period, and have implications for the long-term stability of these metals when sorbed to calcite.

## 2. Materials and methods

### 2.1. Adsorption experiments

The calcite powder used as sorbent in the adsorption experiments was obtained from Spectrum (New Brunswick, New Jersey). The main impurity was Mg, at a concentration of 2800 ppm; the overall heavy metal content of the material was <20 ppm. X-ray diffraction analysis confirmed that the material was calcite, and showed no evidence for the presence of other phases. The calcite powder had an average particle size of 1.8 μm, and a $N_2$-BET surface area of ≅10 $m^2\ g^{-1}$. To avoid calcite dissolution or precipitation during the sorption experiments, we used calcite-water suspensions pre-equilibrated at room temperature and atmospheric $PCO_2$. These suspensions were prepared by pumping water-saturated air through the suspensions, which had calcite particle loadings of 0.1 or 0.5 g calcite $L^{-1}$, for a 2-week period, during which time the suspension pH stabilized at a value of about 8.3. The suspensions were then sealed and subsequently aged for another 4 weeks before reaction with metal. The calcite material partially dissolved during equilibration, in order to achieve the $[Ca^{2+}] = 0.49$ mM equilibrium solution concentration of calcite-saturated solutions of pH 8.3 open to air. As a result, the final particle loadings in the equilibrated suspensions were 0.05 and 0.45 g calcite $L^{-1}$.

Sorption experiments were started by spiking the suspensions with appropriate aliquots of 0.01 M $CuCl_2$, $ZnCl_2$, or $PbCl_2$ stock solutions to give $Cu^{2+}$, $Zn^{2+}$, or $Pb^{2+}$ concentrations of 1.0 or 5.0 μM. Metal addition resulted in a slight drop of the suspension pH (<0.05 pH unit), which was corrected with 0.1 M NaOH within 2 min following metal addition. The samples were then placed on a reciprocal shaker for equilibration for 2 days. After 2 days, the reaction vessels were taken off the shaker for further ageing, and periodically reagitated and measured for pH. The suspension pH values were found to be stable (at pH ≈ 8.3) during the entire reaction period. Subsamples were periodically taken from the main reaction vessels for EXAFS analysis, at reaction times varying from 2 days to 2.5 years. The subsamples were filtered through 0.22 μm filter paper to collect the calcite solids for EXAFS analysis. The wet metal-reacted calcite pastes were loaded into lucite sample holders and sealed with Kapton tape to prevent drying. The EXAFS spectra of these wet samples were collected within 24 h following filtration, and the samples were checked after data collection to confirm that they were still moist. In addition to these wet samples, we also analyzed a number of dried samples. These samples were prepared by air-drying the 2 day samples after they

had been analyzed. Following drying, the samples were stored in sealed containers for approximately 2.5 years before they were reanalyzed by EXAFS. Based on the amount of entrained solute present in the moist samples prior to drying (approximately 1 mL per gram of calcite after filtration), and considering the $Ca^{2+}$ concentration in air-equilibrated calcite solutions of pH 8.3 (0.5 mM), the surface site density of calcite ($5 \times 10^{18}$ sites $m^{-2}$, according to Möller and Sastri, 1974), and the 10 $m^2$ $g^{-1}$ surface areas of the calcite powder used in this study, it was calculated that sample drying potentially could add a calcite monolayer to 0.6% of the calcite surface present in these samples. Considering that the metal loadings in the dried samples were on the order of 12–17% monolayer coverage (as will be shown in the results section), sample drying provided insufficient calcite precipitation to cover sorbed metal and form a metal-calcite solid solution. As a result, sample drying alone would not explain metal incorporation into the calcite lattice if it occurred to a significant extent. EXAFS analysis of the dried samples provided insight into the combined effects of drying and ageing on the speciation of calcite-sorbed $Zn^{2+}$, $Pb^{2+}$, and $Cu^{2+}$, as complementary information to the results of the wet ageing experiments described above.

The calcite metal loadings of the sorption samples were determined following EXAFS analysis. Samples were oven-dried at 60 °C, weighed, and dissolved in 0.2 M $HNO_3$, at a 1:100 solid to liquid weight ratio. The solutes were then analyzed for dissolved $Cu^{2+}$, $Zn^{2+}$, or $Pb^{2+}$ using inductively coupled plasma (ICP) spectrometry, and metal loading was calculated from the solute metal concentration and the amount of calcite solid dissolved.

The reference compounds used in this study were, for $Zn^{2+}$: hydrozincite ($Zn_5(OH)_6(CO_3)_2$), for $Cu^{2+}$: malachite ($Cu_2(OH)_2CO_3$), and for $Pb^{2+}$: $Pb_4(OH)_4{}^{4+}$(aq). EXAFS data of these references were collected and analyzed to evaluate the importance of precipitation reactions in the sorption samples (in the case of $Cu^{2+}$ and $Zn^{2+}$), and to estimate the accuracy of the EXAFS fitting parameters. Additionally, the data of the sorption samples were compared to those of dilute $Cu^{2+}$-, $Zn^{2+}$-, and $Pb^{2+}$-calcite solid solutions to evaluate the possible occurrence of solid solution formation. Preparation of these metal-doped calcites was done using the modified free-drift method described in detail by Paquette and Reeder (1995) and Reeder (1996), and their EXAFS characterization is discussed in Reeder et al. (1999), Elzinga and Reeder (2002), and Rouff et al. (2004).

### 2.2. EXAFS data collection and analysis

EXAFS spectra were recorded on beamlines X-11A and X-18B of the National Synchroton Light Source (NSLS) at Brookhaven National Laboratory. The storage ring operated at 2.84 GeV with a maximum current of 280 mA. A Si(1 1 1) crystal pair (X-11A) or a channel-cut Si(1 1 1) crystal (X-18B) was used in the monochromator, with detuning of 40% for harmonic rejection. The monochromator was calibrated using appropriate metal foils. Multiple scans (15–20 typically) of the $Cu^{2+}$-, $Zn^{2+}$-, and $Pb^{2+}$-calcite adsorption samples, as well as the dilute metal-calcite solid solutions were collected at the Cu and Zn *K*-edges and the Pb $L_3$-edge, using a 13-element Ge solid-state detector for fluorescence detection. The adsorption samples were analyzed at room temperature, whereas the dilute metal-calcite solid solutions were run at liquid nitrogen temperature (77 K). The EXAFS data of the reference compounds were collected in transmission mode at room temperature. Scans were calibrated and averaged prior to fitting. Further data reduction and fitting were performed with the WinXAS2000 software package (Ressler, 1997) using standard procedures.

Theoretical backscattering paths were calculated with FEFF7 (Ankudinov and Rehr, 1997) based on input files of Cu, Zn or Pb substituting in the Ca site in calcite. Fitting was done in *R* space out to approximately 4 Å. For the adsorption samples, no constraints were placed on the fitting parameters of the first-neighbor O shells, but the Debye-Waller factors ($\sigma^2$) of the higher shells were fixed at 0.01 $Å^2$ to reduce the number of free parameters in the fitting procedure. The EXAFS data of the $Zn^{2+}$-, $Cu^{2+}$-, and $Pb^{2+}$-doped calcite samples indicated that these metals occupy the Ca site in the calcite structure. To reduce the number of free parameters in the fitting procedure of these samples, the coordination numbers of the shells surrounding incorporated metal atoms were therefore fixed at values consistent with substitution in Ca sites, whereas all other parameters were allowed to vary. The number of parameters allowed to vary never exceeded the Nyquist limit. Error estimates are ±0.02 Å for the radial distance (*R*) values of the first shells, and ±0.05 Å for higher shells. For the coordination number (CN), which is correlated to the Debye-Waller factor, the error is estimated at ±15% for the first O shell, and >25% for the further shells.

## 3. Results

The raw and fitted $k^3$-weighted $\chi$ spectra of the metal-calcite adsorption samples of various reaction times are shown in Figs. 1–3, along with the corresponding radial structure functions obtained by Fourier transformation of the raw $\chi$ spectra. Also shown are the EXAFS data of the various reference compounds. Included for the sorption samples shown in Figs. 1–3 is the metal surface loading (reported as fraction of Ca surface sites occupied) for each sample. The analyses of the calcite metal loadings indicated that metal uptake by calcite proceeded rapidly under the conditions used, with ⩾90% of total metal removed from solution within 48 h (the first time point of sampling) in all cases. Due to this fast, extensive metal uptake, no significant additional adsorption occurred after the first sampling time point, and as a result, the samples analyzed as part of the reaction time sequence had similar metal loadings (Figs. 1–3). Consequently, this study isolates the effect

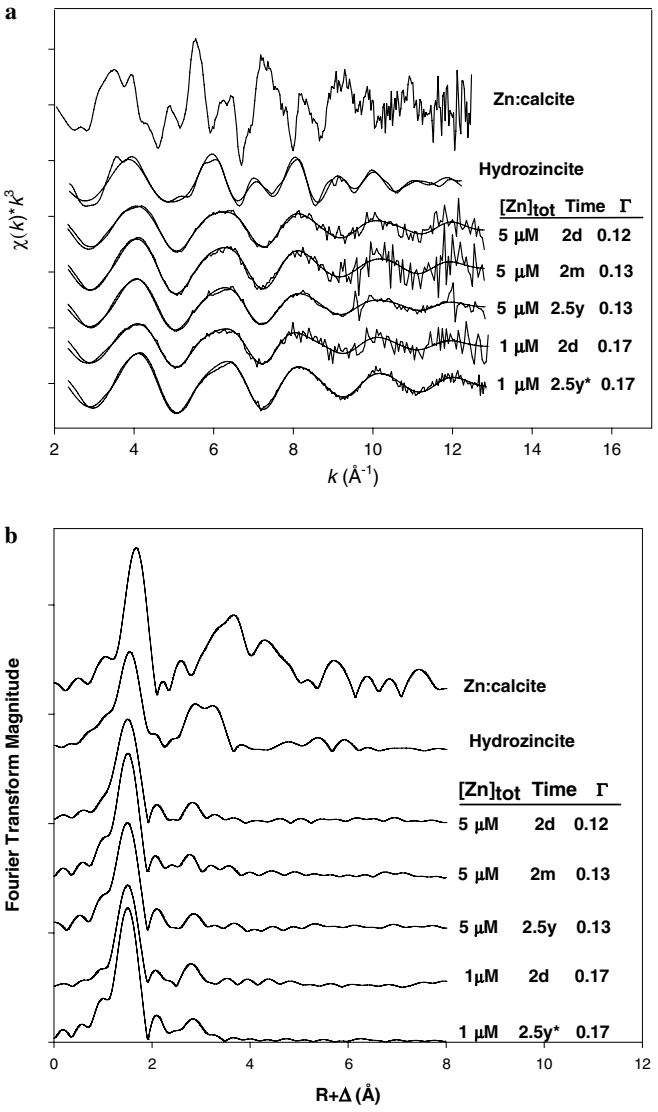


Fig. 1. (a) Raw and fitted $k^3$-weighted $\chi$ functions of $Zn^{2+}$-calcite sorption samples and $Zn^{2+}$ reference compounds. (b) Fourier transforms of $Zn^{2+}$ sorption samples and references, obtained by Fourier-transformation of the $k^3$-weighted $\chi$ function of the raw data shown in (a). *Dried sample, subsequently aged for 2.5 years; $\Gamma$ is the metal surface coverage, expressed as fraction of monolayer coverage.

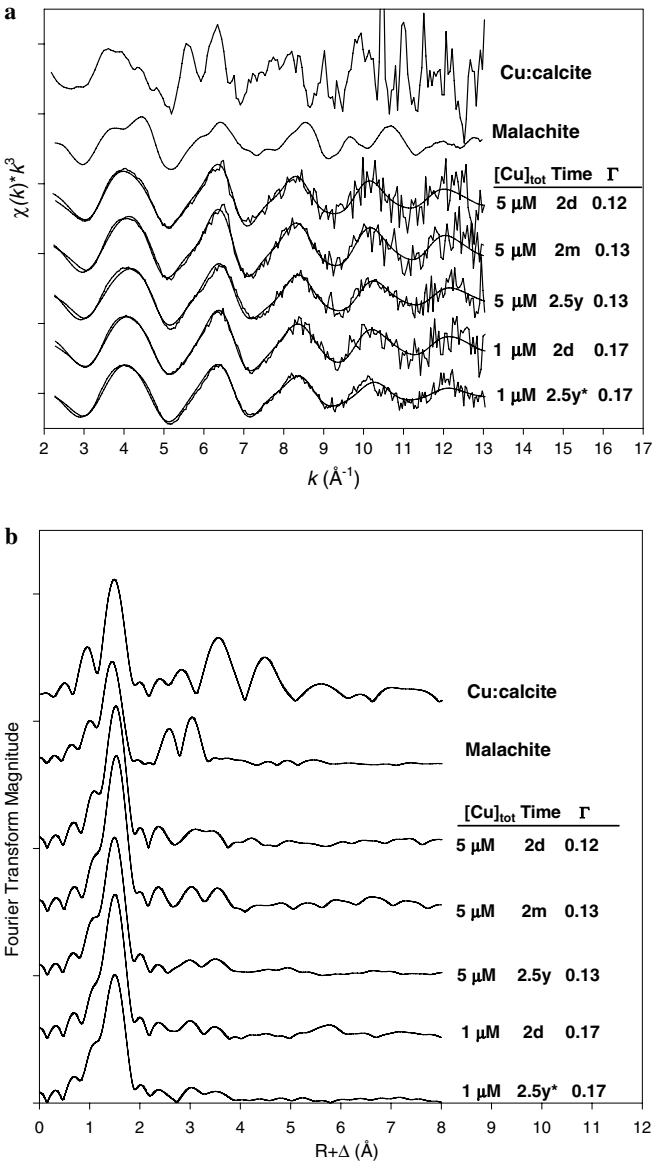


Fig. 2. (a) Raw and fitted $k^3$-weighted $\chi$ functions of $Cu^{2+}$-calcite sorption samples and $Cu^{2+}$ reference compounds. (b) Fourier transforms of $Cu^{2+}$ sorption samples and references, obtained by Fourier-transformation of the $k^3$-weighted $\chi$ function of the raw data shown in (a). *Dried sample, subsequently aged for 2.5 years; $\Gamma$ is the metal surface coverage, expressed as fraction of monolayer coverage.

of ageing on the speciation of $Cu^{2+}$, $Zn^{2+}$, and $Pb^{2+}$ initially bound at the calcite surface as probed by EXAFS, i.e., any changes observed in the speciation of these sorbed metals over time would reflect a reaction time effect, and would not be due to changes in the metal surface loadings.

For all three metals, the EXAFS data obtained for the adsorption samples are markedly different from those of the solid standards, indicating that precipitation of these metal phases had not occurred to any significant extent in these experiments. Although the 5 μM $Cu^{2+}$ and $Zn^{2+}$ samples were initially slightly oversaturated with respect to malachite and hydrozincite (saturation index = 0.56 and 0.23, respectively, as determined from speciation calculations with the PHREEQC speciation program), the metal concentrations in solution at all sampling time points were below the solubilities of these precipitate phases, as determined from the amount of metal sorbed. The absence of these precipitates in the sorption samples despite initial oversaturation indicates that metal removal from solution via adsorption reactions out-competed precipitate formation under the given conditions. In the $Pb^{2+}$ experiments, only 1 μM $Pb^{2+}$ concentrations were used, and PHREEQC calculations indicated undersaturation with respect to any $Pb^{2+}$ precipitates at this concentration. The data for the metal-calcite sorption samples shown in Figs. 1–3 are therefore representative of calcite-associated $Cu^{2+}$, $Zn^{2+}$, and $Pb^{2+}$ atoms, with negligible contributions from metal entrapped in secondary precipitates.

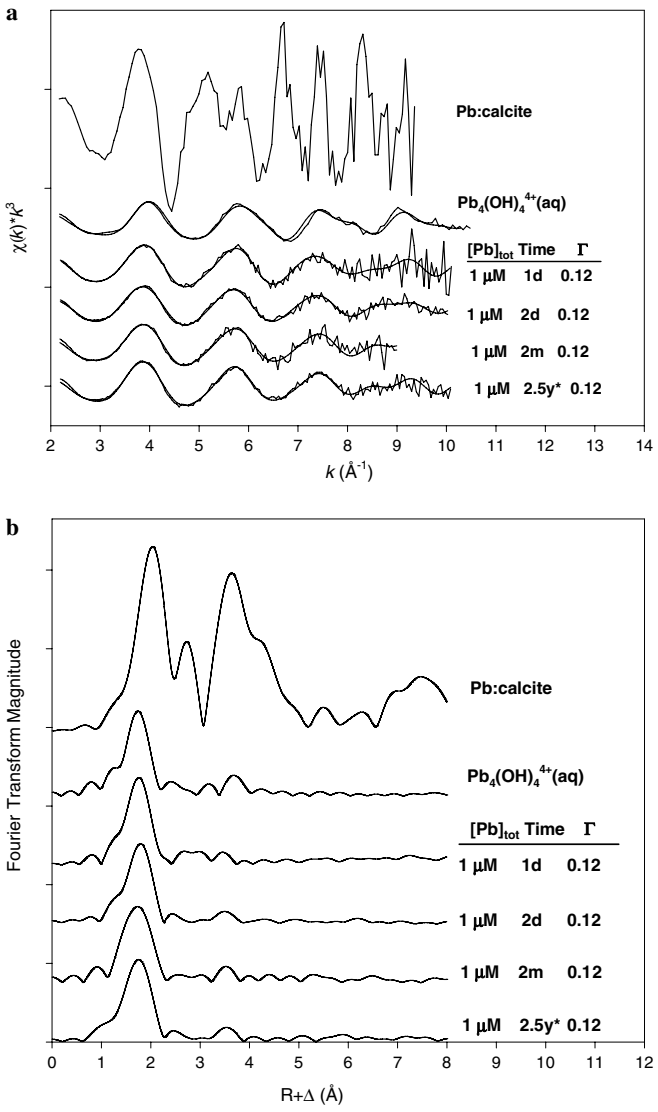


Fig. 3. (a) Raw and fitted $k^3$-weighted $\chi$ functions of $Pb^{2+}$-calcite sorption samples and $Pb^{2+}$ reference compounds. (b) Fourier transforms of $Pb^{2+}$ sorption samples and references, obtained by Fourier-transformation of the $k^3$-weighted $\chi$ function of the raw data shown in (a). *Dried sample, subsequently aged for 2.5 years; $\Gamma$ is the metal surface coverage, expressed as fraction of monolayer coverage.

Addition of $Cu^{2+}$, $Zn^{2+}$, and $Pb^{2+}$ to the saturated calcite-water suspensions likely resulted in (slight) supersaturation with respect to $Cu^{2+}$-calcite, $Zn^{2+}$-calcite, and $Pb^{2+}$-calcite solid solutions over a range of different compositions, as discussed in Tesoriero and Pankow (1996), Prieto et al. (2003), and Astilleros et al. (2002, 2003a,b). Due to the lack of suitable models for $Cu^{2+}$, $Zn^{2+}$ and $Pb^{2+}$ substitution in calcite, it is not possible to provide a reliable estimate of the degree of supersaturation of such phases. As discussed below, however, substantial differences in coordination allow us to distinguish between coprecipitated and adsorbed $Cu^{2+}$, $Zn^{2+}$, and $Pb^{2+}$ using EXAFS.

The EXAFS fitting results of the various samples are presented in Table 1. The EXAFS of the metal-calcite sorption samples are dominated by scattering from first-shell oxygens atoms, which are located at a radial distance of ~1.95 Å for $Cu^{2+}$ and $Zn^{2+}$, and at ~2.34 Å in the case of $Pb^{2+}$ (Figs. 1–3, Table 1). Shells appearing at longer radial distances in the RSFs (Figs. 1–3) were successfully fitted with scattering from C, O, and Ca atoms (Table 1), consistent with results from previous studies (Elzinga and Reeder, 2002; Rouff et al., 2004; Lee et al., 2005). The fitting results indicate the formation of mononuclear inner-sphere $Cu^{2+}$, $Zn^{2+}$, and $Pb^{2+}$ adsorption complexes positioned in Ca sites at the calcite surface, which are linked to the calcite surface by coordinating to surface carbonate groups. The observed first-shell Zn–O distance of 1.95 Å indicates that $Zn^{2+}$ assumes a tetrahedral configuration with respect to first-shell O when it adsorbs to the calcite surface (Elzinga and Reeder, 2002). Copper adsorbs as a Jahn–Teller distorted octahedron, with the (close) equatorial O atoms located at ~1.95 Å from the $Cu^{2+}$ center, whereas the axial O atoms, located at longer radial distances, could not be reliably fitted, most likely due to high structural and/or thermal disorder in this correlation (Elzinga and Reeder, 2002; Lee et al., 2005). The Pb–O first-shell distance of 2.34 Å indicates that the $Pb^{2+}$-calcite adsorption complex has a distorted trigonal pyramidal or square pyramidal first O shell, with an active lone pair of electrons forcing the O atoms towards one side of the $Pb^{2+}$ atom (Rouff et al., 2004). The same type of first-shell Pb–O coordination occurs in the $Pb_4(OH)_4^{4+}$(aq) reference sample (Table 1), and has been observed for inner-sphere $Pb^{2+}$ adsorption complexes formed at Ru(IV)-, Fe(III)-, Al(III)-, and Mn(III, IV)-(hydr)oxide surfaces (Bargar et al., 1997a,b; Strawn et al., 1998; Matocha et al., 2001; Trivedi et al., 2003; Scheckel et al., 2004). Possible linkages between sorbed $Cu^{2+}$, $Zn^{2+}$, and $Pb^{2+}$ ions and the calcite surface that are consistent with the EXAFS fitting results are presented in Fig. 4; a more extended view of the coordination of these metals at the calcite surface is provided in Elzinga and Reeder (2002) and Rouff et al. (2004).

The EXAFS data of sorption samples reacted for different times are essentially the same (Figs. 1–3), indicating that the average local coordination environments of sorbed $Cu^{2+}$, $Zn^{2+}$, and $Pb^{2+}$ did not significantly change over time. The coordination environments of $Cu^{2+}$, $Zn^{2+}$, and $Pb^{2+}$ incorporated in the calcite structure are noticeably different from those of the surface complexes of these metals when adsorbed at the calcite surface, as evidenced by comparison of the EXAFS data of the dilute metal-calcite solid solutions and the metal-calcite sorption samples. Incorporated $Cu^{2+}$, $Zn^{2+}$, and $Pb^{2+}$ all occupy the $Ca^{2+}$ site within the calcite structure, and are in octahedral coordination with respect to first-shell O, as indicated by first-shell O distances of 2.01, 2.13, and 2.52 Å for $Cu^{2+}$, $Zn^{2+}$, and $Pb^{2+}$, respectively (Table 1), which are significantly different from the first-shell O distances observed for adsorbed $Cu^{2+}$ (1.95 Å), $Zn^{2+}$ (1.95 Å), and $Pb^{2+}$ (2.34 Å) surface complexes (Table 1). This difference in first-shell O coordination facilitates discrimination between

Table 1
EXAFS fitting results for the various metal-calcite sorption samples and reference materials

| Zn sorption samples | | | | | | | Pb sorption samples | | | | | | |
|---|---|---|---|---|---|---|---|---|---|---|---|---|---|
| $[Zn]_{tot}$ (μM) | Time | $\Gamma$ | Shell | CN | $R$ (Å) | $\sigma^2$ (Å$^2$) | $[Pb]_{tot}$ (μM) | Time | $\Gamma$ | Shell | CN | $R$ (Å) | $\sigma^2$ (Å$^2$) |
| 5 | 2 days | 0.12 | Zn–O | 3.7 | 1.96 | 0.007 | 1 | 1 day | 0.12 | Pb–O | 4.3 | 2.34 | 0.014 |
| | | | Zn–C | 3.6 | 2.82 | 0.01[b] | | | | Pb–C | 3.3 | 3.29 | 0.01[b] |
| | | | Zn–O | 1.9 | 3.01 | 0.01[b] | | | | Pb–O | 3.8 | 3.62 | 0.01[b] |
| | | | Zn–Ca | 1.0 | 3.34 | 0.01[b] | | | | Pb–Ca | 1.4 | 3.98 | 0.01[b] |
| 5 | 2 months | 0.13 | Zn–O | 4.2 | 1.96 | 0.007 | 1 | 2 days | 0.12 | Pb–O | 4.3 | 2.35 | 0.013 |
| | | | Zn–C | 3.4 | 2.83 | 0.01[b] | | | | Pb–C | 1.8 | 3.33 | 0.01[b] |
| | | | Zn–O | 1.2 | 3.05 | 0.01[b] | | | | Pb–O | 2.0 | 3.58 | 0.01[b] |
| | | | Zn–Ca | 0.9 | 3.33 | 0.01[b] | | | | Pb–Ca | 1.0 | 3.98 | 0.01[b] |
| 5 | 2.5 years | 0.13 | Zn–O | 4.2 | 1.95 | 0.008 | 1 | 2 months | 0.12 | Pb–O | 4.7 | 2.34 | 0.013 |
| | | | Zn–C | 2.8 | 2.83 | 0.01[b] | | | | Pb–C | 2.4 | 3.33 | 0.01[b] |
| | | | Zn–O | 1.1 | 3.04 | 0.01[b] | | | | Pb–O | 3.1 | 3.57 | 0.01[b] |
| | | | Zn–Ca | 0.9 | 3.36 | 0.01[b] | | | | Pb–Ca | 1.5 | 3.97 | 0.01[b] |
| 1 | 2 days | 0.17 | Zn–O | 3.6 | 1.96 | 0.008 | 1 | 2.5 years[a] | 0.12 | Pb–O | 4.5 | 2.34 | 0.013 |
| | | | Zn–C | 2.2 | 2.86 | 0.01[b] | | | | Pb–C | 1.4 | 3.36 | 0.01[b] |
| | | | Zn–O | 1.2 | 3.08 | 0.01[b] | | | | Pb–O | 2.1 | 3.61 | 0.01[b] |
| | | | Zn–Ca | 1.0 | 3.34 | 0.01[b] | | | | Pb–Ca | 1.3 | 3.99 | 0.01[b] |
| 1 | 2.5 years[a] | 0.17 | Zn–O | 4.5 | 1.95 | 0.007 | | | | | | | |
| | | | Zn–C | 2.5 | 2.82 | 0.01[b] | | | | | | | |
| | | | Zn–O | 1.1 | 3.10 | 0.01[b] | | | | | | | |
| | | | Zn–Ca | 1.0 | 3.35 | 0.01[b] | | | | | | | |

| Cu sorption samples | | | | | | | Reference samples | | | | |
|---|---|---|---|---|---|---|---|---|---|---|---|
| $[Cu]_{tot}$ (μM) | Time | $\Gamma$ | Shell | CN | $R$ (Å) | $\sigma^2$ (Å$^2$) | | Shell | CN | $R$ (Å) | $\sigma^2$ (Å$^2$) |
| 5 | 2 days | 0.12 | Cu–O | 4.1 | 1.96 | 0.005 | Hydrozincite | Zn–O | 5.3 | 2.03 | 0.011 |
| | | | Cu–C | 2.6 | 2.95 | 0.01[b] | | Zn–Zn | 2.1 | 3.15 | 0.012 |
| | | | Cu–O | 1.5 | 3.35 | 0.01[b] | | Zn–Zn | 3.4 | 3.54 | 0.009 |
| | | | Cu–Ca | 1.8 | 3.90 | 0.01[b] | | | | | |
| | | | | | | | $Zn_xCa_{(1-x)}CO_3$ | Zn–O | 6.3 | 2.13 | 0.008 |
| 5 | 2 months | 0.13 | Cu–O | 4.1 | 1.96 | 0.005 | | Zn–C | 6[b] | 3.13 | 0.005 |
| | | | Cu–C | 2.3 | 2.93 | 0.01[b] | | Zn–O | 6[b] | 3.36 | 0.006 |
| | | | Cu–O | 2.4 | 3.30 | 0.01[b] | | Zn–Ca | 6[b] | 3.95 | 0.005 |
| | | | Cu–Ca | 2.3 | 3.81 | 0.01[b] | | | | | |
| | | | | | | | Malachite | Cu–O | 3.4 | 1.93 | 0.008 |
| 5 | 2.5 years | 0.13 | Cu–O | 4.1 | 1.94 | 0.006 | | | | | |
| | | | Cu–C | 1.7 | 2.93 | 0.01[b] | $Cu_xCa_{(1-x)}CO_3$ | Cu–O | 4.1 | 2.01 | 0.006 |
| | | | Cu–O | 0.8 | 3.29 | 0.01[b] | | Cu–C | 6[b] | 2.99 | 0.007 |
| | | | Cu–Ca | 1.7 | 3.87 | 0.01[b] | | Cu–O | 6[b] | 3.21 | 0.015 |
| | | | | | | | | Cu–Ca | 6[b] | 3.97 | 0.007 |
| 1 | 2 days | 0.17 | Cu–O | 4.4 | 1.94 | 0.006 | | | | | |
| | | | Cu–C | 2.6 | 2.95 | 0.01[b] | $Pb_4(OH)_4^{4+}$(aq) | Pb–O | 2.2 | 2.28 | 0.008 |
| | | | Cu–O | 1.2 | 3.30 | 0.01[b] | | Pb–Pb | 1.7 | 3.77 | 0.01 |
| | | | Cu–Ca | 1.2 | 3.89 | 0.01[b] | | | | | |
| | | | | | | | $Pb_xCa_{(1-x)}CO_3$ | Pb–O | 6 | 2.51 | 0.005 |
| 1 | 2.5 years[a] | 0.17 | Cu–O | 4.6 | 1.95 | 0.007 | | Pb–C | 6[b] | 3.24 | 0.004 |
| | | | Cu–C | 1.4 | 2.90 | 0.01[b] | | Pb–O | 6[b] | 3.81 | 0.007 |
| | | | Cu–O | 1.6 | 3.32 | 0.01[b] | | Pb–Ca | 6[b] | 4.08 | 0.004 |
| | | | Cu–Ca | 1.4 | 3.82 | 0.01[b] | | | | | |

[a] Dried samples subsequently aged for 2.5 years.
[b] Fixed parameters.

surface-bound (i.e., adsorbed) and lattice-incorporated $Cu^{2+}$, $Zn^{2+}$, and $Pb^{2+}$. The EXAFS results of the sorption samples are therefore inconsistent with metal incorporation into the calcite lattice during reaction, since incorporated metals are expected to have a sixfold (octahedral) coordination with respect to first-shell O, as is observed for the dilute metal-calcite solid solutions presented in Figs. 1–3, whereas none of the sorption samples shows evidence for such a metal coordination. Instead, the metals studied here appear to remain predominantly bonded as tetrahedral $Zn^{2+}$, Jahn–Teller distorted $Cu^{2+}$, and trigonal- or square-pyramidal $Pb^{2+}$ surface complexes, even after

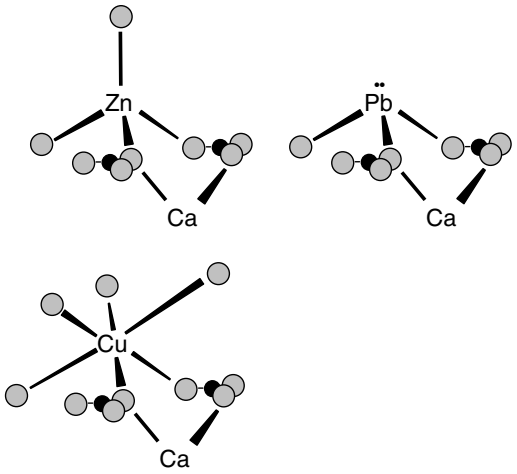


Fig. 4. Linkages between adsorbed $Zn^{2+}$, $Pb^{2+}$, and $Cu^{2+}$ ions and the calcite surface that are consistent with the EXAFS fitting results. Grey and black circles represent O and C atoms, respectively.

sorption times of 2.5 years. Furthermore, sample drying (and subsequent ageing) appears to have no effect on the bonding characteristics of the metal-calcite sorption complexes either, as evidenced by the observation that the EXAFS data of the dried $Cu^{2+}$, $Zn^{2+}$, and $Pb^{2+}$ samples are identical to those of the wet samples. This indicates that in these dried and aged samples, the metals are coordinated in the same way as in the short-term (2 days) experiments performed under wet conditions.

## 4. Discussion

Our EXAFS data indicate that inner-sphere $Cu^{2+}$, $Zn^{2+}$, and $Pb^{2+}$ adsorption complexes formed at the calcite surface after one day remain largely unchanged during 2.5 years of ageing in calcite-water suspensions of pH 8.3 that remain at bulk saturation equilibrium. Adsorption complexes are expected to be more labile compared to incorporated and precipitated metal species, in that they are relatively easily desorbed when changes in solution chemistry disrupt the sorption equilibrium. Mononuclear $Pb^{2+}$ atoms adsorbed as inner-sphere complexes at $\gamma$-$Al_2O_3$ and goethite surfaces, for instance, were found to be bound in a largely reversible fashion: desorption occurred readily and extensively when the metal-reacted solids were contacted with metal-free solutions, indicating that the surface-sorbed $Pb^{2+}$ cations were available for exchange (Strawn et al., 1998; Eick et al., 1999). Moreover, the rate of $Pb^{2+}$ desorption from goethite did not significantly change during a 12 d reaction period (Eick et al., 1999), and in the case of $Pb^{2+}$ sorption to alumina, EXAFS results indicated that the speciation of adsorbed $Pb^{2+}$ did not change during 23 days of reaction (Strawn et al., 1998), suggesting that reaction time had no effect on the potential for $Pb^{2+}$ remobilization.

Rouff et al. (2005) observed that $Pb^{2+}$ sorbs to calcite as a combination of inner-sphere adsorption complexes and lattice-incorporated $Pb^{2+}$ when adsorbed from pre-equilibrated calcite solutions of pH 9.4 and 7.3, as determined by EXAFS spectroscopy. The percentage of incorporated $Pb^{2+}$ values correlated well with the decrease in reversibility of $Pb^{2+}$ sorption at pH 9.4 and 7.3 relative to pH 8.3, where $Pb^{2+}$ sorption was fully reversible and $Pb^{2+}$ was found to be predominantly bonded as an inner-sphere adsorption surface complex with the same configuration found here (Rouff et al., 2005). Zachara et al. (1991) attributed observed partial irreversibility of divalent metal sorption to calcite to solid solution formation, as the irreversibility of metal sorption increased for metals having ionic radii similar to that of $Ca^{2+}$. Our current findings suggest that the lability of $Cu^{2+}$, $Zn^{2+}$, and $Pb^{2+}$ atoms sorbed to calcite does not significantly change over time, i.e., there is no spectroscopic evidence to indicate that during sample ageing the inner-sphere adsorbed metal complexes transform into more stable (or less labile) metal-calcite complexes that are less susceptible to desorption, such as lattice-incorporated metal ions or metal precipitate phases. Similarly, sample drying followed by 2.5 years of ageing seems to have no effect on the metal surface complex characteristics as seen using EXAFS, suggesting that the combination of drying and ageing has no significant effect on the coordination of the metal sorbates either.

It should be noted that the results reported here are likely to be at least partially conditional on the experimental procedures used. In this study, we used calcite–water suspensions that were equilibrated before metal sorption was allowed to take place; moreover, bulk equilibrium with respect to calcite was maintained during the entire 2.5-year reaction period used. It is quite conceivable that different results would have been found if at any time during the 2.5 years of reaction the calcite bulk equilibrium had been perturbed (due to changes in temperature or solution composition for instance), as a result of which calcite dissolution and (re)precipitation could occur. Since all three of the metals used in this study can substitute for Ca atoms in the calcite lattice, any calcite dissolution and recrystallization occurring when these metals are present would likely result in at least some metal-calcite solid solution formation. Additionally, the experiments were done at essentially constant metal loadings, due to the fact that no additional metal uptake occurred after the first sampling time point; as a result, this study isolates the effect of ageing on the speciation of calcite-sorbed $Cu^{2+}$, $Zn^{2+}$, and $Pb^{2+}$. In experimental systems where there is continued loading of the calcite surface over time, the operation of different or additional mechanism(s) of metal uptake would not be unlikely.

In the following, the results from this study are compared to those of previous investigations dealing with divalent metal uptake by calcite. Particular focus is placed on differences in experimental procedures, which appear to play an important role in the observed mechanisms of metal uptake by calcite as a function of reaction time.

The persistence of surface-adsorbed species with time observed here under both wet and dry conditions is notable

in view of results from previous studies of metal sorption to calcite, where formation of metal-calcite solid solutions was observed for $Cu^{2+}$, $Cd^{2+}$, and $Zn^{2+}$ following deposition of these metals on the calcite surface (Stipp et al., 1992; Stipp, 1994, 1998; Schosseler et al., 1999). There are several important differences in the experimental conditions used in these studies versus ours that may account for these different findings. Schosseler et al. (1999) observed a transformation of calcite-sorbed $Cu^{2+}$ surface complexes into lattice-incorporated $Cu^{2+}$ species over time using time-resolved EPR spectroscopy. Unlike our experiments, the solutions used in this study were under-saturated with respect to calcite before reaction with $Cu^{2+}$ was started. As a result, the calcite material in the Schosseler et al. (1999) experiments likely underwent active dissolution and recrystallization following $Cu^{2+}$ introduction, which may explain the incorporation of $Cu^{2+}$ into the near-surface calcite lattice following initial coordination at surface sites. In our experiments, calcite-saturated solutions were used, and, as a result, no net calcite dissolution and precipitation occurred during reaction with $Cu^{2+}$, which may have prevented the incorporation of $Cu^{2+}$ via surface recrystallization.

Stipp et al. (1992) and Stipp (1994, 1998) observed a loss of $Cd^{2+}$ and $Zn^{2+}$ from the calcite surface based on time-resolved XPS and LEED experiments over time scales as short as a few days under both wet and dry conditions, and interpreted this loss as due to solid-state diffusion of $Cd^{2+}$ and $Zn^{2+}$ into the bulk structure. These studies (performed under ambient conditions of temperature and pressure) employed freshly cleaved calcite $(10\bar{1}4)$ faces exposed to metal-bearing solutions that were not in equilibrium with calcite. The use of aged calcite powder in our study versus freshly cleaved single crystals may have resulted in different mechanisms of metal adsorption between these experiments, thereby possibly affecting the potential for metal mobility. Ageing of the calcite powder in solution, as done in our experiments, may have "healed" the calcite surface from highly reactive surface defect sites that are likely to be present on freshly cleaved crystal faces, and this treatment may have resulted in differences in the types of calcite surface sites available for $Zn^{2+}$ complexation between these experiments. Additionally, as mentioned earlier, non-equilibrated solutions, as used in the Stipp et al. experiments, may affect the calcite surface properties and behavior relative to systems employing equilibrated solutions without net calcite dissolution or precipitation, thereby affecting the mechanism and possibly the stability of metal coordination.

Mechanistic differences in metal coordination may be of particular importance in the case of $Zn^{2+}$ and $Pb^{2+}$, for which we observe surface complexes that have substantially different first-shell O configurations than their octahedrally coordinated counterparts in bulk calcite. A more subtle but still notable difference in first-shell O coordination between bulk and surface species is observed for $Cu^{2+}$. If solid-state diffusion were operative, the change in O-shell coordination required during transition of the metal from the surface into the bulk would likely obstruct movement of adsorbed $Zn^{2+}$, $Pb^{2+}$, and $Cu^{2+}$ in our experiments, whereas such a coordination change may not have been required for the conditions in the experiments of Stipp et al. (1992) and Stipp (1994, 1998). For instance, a combined X-ray standing wave and surface EXAFS study by Cheng et al. (1998) indicated the incorporation of $Zn^{2+}$ as an octahedral complex at the calcite $(10\bar{1}4)$ surface by direct substitution for surface Ca atoms. As in the Stipp et al. (1992) and Stipp (1994, 1998) experiments, the Cheng et al. (1998) study employed freshly cleaved single crystals that were exposed to $Zn^{2+}$-bearing solutions that were not in equilibrium with calcite. If solid-state diffusion were an operative mechanism in metal sequestration by calcite under ambient conditions, it is reasonable to expect that the formation of octahedral $Zn^{2+}$ surface complexes would facilitate movement of $Zn^{2+}$ into the bulk, whereas the tetrahedral coordination we observe in our powder experiments would likely hinder $Zn^{2+}$ movement. A recent XPS study by Chada et al. (2005) revealed no evidence to suggest solid-state diffusion of $Cd^{2+}$ and $Pb^{2+}$ deposited onto single crystal calcite $(10\bar{1}4)$ surfaces from pre-equilibrated calcite solutions, further indicating that differences in experimental setup and conditions may affect the coordination and associated stability of surface-sorbed metal species.

Additional complexity arises from the fact that different metals may exhibit different behavior, as demonstrated by a recent study of Hoffmann and Stipp (2001) on $Ni^{2+}$ uptake by calcite single crystals. In contrast to $Zn^{2+}$ and $Cd^{2+}$, $Ni^{2+}$ did not show evidence for loss from the surface, interpreted as a lack of solid-state diffusion into the calcite bulk, although the same experimental methods and materials were used as in the earlier studies dealing with $Zn^{2+}$ and $Cd^{2+}$ uptake. Further studies on the relation between the characteristics of metal coordination and the potential for metal solid diffusion would be useful, as would be studies on the influence of experimental parameters such as the pH and calcite saturation state of reacting solutes, the (calcite) surface roughness, and the possible effect of surface site characteristics on this process.

The results from this study also allow comment on the influence of the dynamic equilibrium processes occurring at the calcite surface on long-term metal sorption. At saturation, steady-state dynamic exchange between surface and solution species occurs at the calcite-water interface, resulting in a situation of dynamic equilibrium. Studies by Van der Weijden et al. (1994, 1997a,b) indicated that as a result of these steady-state dissolution and precipitation processes, Ca atoms may exchange into the near-surface calcite lattice, as determined via $^{45}Ca$ exchange experiments. It is therefore interesting to note that no detectable incorporation of $Cu^{2+}$, $Zn^{2+}$, and $Pb^{2+}$ into the calcite structure occurs, in spite of the fact that these metals are able to substitute for $Ca^{2+}$ atoms in the calcite lattice. The lack of noticeable metal incorporation even after extended sorption times may be due to inhibition or attenuation of the dynamic exchange processes at the calcite surface following

metal sorption. Interaction of metal impurities with calcite kinks and steps, where most of the dynamic exchange reactions occur, has been shown to inhibit both calcite growth and dissolution, which is attributed to blocking of these high energy sites (e.g. Meyer, 1984; Lea et al., 2001). Therefore, inner-sphere metal sorption is likely to inhibit steady-state exchange between the aqueous and solid phase, thereby reducing the microscopic dissolution and precipitation reactions that are likely to be required for metal incorporation into the near-surface lattice, and thus obstructing the subsequent formation of metal-calcite solid solutions. The inhibition of calcite growth and dissolution may be particularly effective for the three metals studied here, as a result of their non-octahedral coordination at calcite surface sites and their high affinity for the calcite surface.

Of further note is that the $^{45}Ca$ exchange results reported by Van der Weijden et al. (1994, 1997a,b) indicated that the steady-state flux between the solid and aqueous phase was lowest at pH 8.4, and increased at both lower and higher pH values in the pH range 7.4–9.0. The inherently low exchange rates between the aqueous and solid phase in our studies (at pH 8.3) may have furthered the inhibitory effect of metal sorption on the steady-state exchange processes between the solid and aqueous phase, thereby effectively obstructing metal incorporation. Results from a recent study by Rouff et al. (2005) on pH-dependent $Pb^{2+}$ uptake mechanisms by calcite are consistent with this notion, as $Pb^{2+}$ lattice incorporation was observed at pH 7.3 and 9.4, where exchange rates are relatively high, whereas only $Pb^{2+}$ adsorption was observed at pH 8.3, where exchange rates are lowest.

The results of Van der Weijden et al. (1994, 1997a) indicated that the ''surface recrystallization'' of calcite occurring slowly as a result of the microscopic dissolution and precipitation reactions associated with steady-state exchange between the aqueous and solid phase, may lead to slow incorporation of $Cd^{2+}$ into the near-surface calcite lattice, as evidenced by a decrease in reversibility of $Cd^{2+}$ sorption over time. These experiments were done in a similar fashion as ours, using pre-equilibrated calcite-suspensions, and maintaining calcite saturation during the entire reaction time frame. Incorporation of $Cd^{2+}$ may be more facile than for $Zn^{2+}$, $Pb^{2+}$, and $Cu^{2+}$, as $Cd^{2+}$ has an ionic radius more similar to that of $Ca^{2+}$, and, unlike the other three metals, is likely to coordinate at the calcite surface as an octahedral complex (Elzinga and Reeder, 2002). As a result, the inhibitory effect of $Cd^{2+}$ on the steady-state microscopic dissolution and precipitation processes is expected to be less than for $Zn^{2+}$, $Pb^{2+}$, and $Cu^{2+}$, making lattice incorporation of $Cd^{2+}$ over long sorption times perhaps more likely than for these other divalent metals. In support of this hypothesis, the results of Meyer (1984) indicated that the inhibitory effect of $Zn^{2+}$ and $Pb^{2+}$ on calcite growth was much greater than for $Cd^{2+}$. However, incorporation of $Cd^{2+}$ into the calcite structure during long-term sorption experiments, as alluded to in the experiments of Van der Weijden et al. (1994, 1997a), remains to be spectroscopically confirmed.

## 5. Conclusions

This study examined the effect of ageing on the speciation of $Zn^{2+}$, $Pb^{2+}$, and $Cu^{2+}$ sorbed at the calcite surface over a 2.5-year reaction period, employing extended X-ray absorption fine structure (EXAFS) spectroscopy to characterize metal speciation on the molecular scale. Experiments were performed using pre-equilibrated calcite-water suspensions of pH 8.3, at metal concentrations below the solubility of metal hydroxide and carbonate precipitates, and at constant surface metal loadings. The EXAFS results showed that no significant changes in the mode of metal coordination occurred over time, and indicated that all three metals remained coordinated at the calcite surface as inner-sphere sorption complexes, with no evidence to suggest slow formation of dilute metal-calcite solid under the reaction conditions employed. All three metals studied here assume a non-octahedral configuration with respect to first-shell O when coordinating to the calcite surface, with $Zn^{2+}$ adsorbing as a tetrahedral complex, $Cu^{2+}$ as a Jahn–Teller distorted complex, and $Pb^{2+}$ coordinating as a trigonal- or square-pyramidal surface complex. The non-octahedral configuration of these surface complexes may have hindered movement of the metals into the calcite structure, where $Ca^{2+}$ is in octahedral coordination with first-shell O. The use of pre-equilibrated calcite suspensions, with no net calcite dissolution or precipitation, likely prevented metal incorporation into the lattice via surface recrystallization. The results from this study imply that ageing alone does not increase the stability of $Zn^{2+}$, $Pb^{2+}$, and $Cu^{2+}$ partitioning to calcite; rather, under the given conditions, these metals appear to remain available for exchange even after extended sorption times. These results may be (partially) specific to the conditions used in these experiments, where calcite saturation (at pH 8.3) was maintained during the entire 2.5-year reaction period, and the metal surface loadings were constant over time. Disruption of the calcite equilibrium, leading to calcite dissolution and recrystallization in the presence of these divalent metals, likely would have resulted in some metal-calcite solid solution formation. Additionally, continued loading of the calcite surface with metal could conceivably lead to different or additional modes of metal uptake. However, the results from the present study show that in the absence of such processes, sorbed $Zn^{2+}$, $Pb^{2+}$, and $Cu^{2+}$ remain coordinated at the calcite surface as mononuclear inner-sphere complexes during extended reaction periods.

## Acknowledgments

This research was supported by the Center for Environmental Molecular Science through NSF Grant

CHE-0221934 and by NSF Grant EAR-0207756. The authors thank Dr. Roy Wogelius and three anonymous reviewers for comments that improved this manuscript, Dr. K. Nagy (University of Illinois at Chicago) for providing access to ICP spectrometry equipment, and the personnel at NSLS beamlines X11A and X18B for assistance with EXAFS data collection.

*Associate editor:* Roy A. Wogelius

## References

Ainsworth, C.C., Pilon, J.L., Gassman, P.L., Van der Sluys, W.G., 1994. Cobalt, cadmium, and lead sorption to hydrous iron oxide: residence time effect. *Soil Sci. Soc. Am. J.* **58**, 1615–1623.

Ankudinov, A.L., Rehr, J.J., 1997. Relativistic spin-dependent X-ray sorption theory. *Phys. Rev. B* **56**, R1712–R1715.

Arai, Y., Sparks, D.L., 2002. Residence time effects on arsenate surface speciation at the aluminum oxide–water interface. *Soil Sci.* **167**, 303–314.

Astilleros, J.M., Pina, C.M., Fernández-Díáz, L., Putnis, A., 2002. Molecular scale surface processes during the growth of calcite in the presence of manganese. *Geochim. Cosmochim. Acta* **66**, 3177–3189.

Astilleros, J.M., Pina, C.M., Fernández-Diáz, L., Putnis, A., 2003a. Supersaturation functions in binary solid-solution-aqueous solution systems. *Geochim. Cosmochim. Acta* **67**, 1601–1608.

Astilleros, J.M., Pina, C.M., Fernández-Diáz, L., Putnis, A., 2003b. Metastable phenomena on calcite {1014} surfaces growing from $Sr^{2+}$-$Ca^{2+}$- $CO_3^{2-}$ aqueous solutions. *Chem. Geol.* **193**, 93–107.

Bargar, J.R., Brown Jr., G.E., Parks, G.A., 1997a. Surface complexation of Pb(II) at oxide–water interfaces. I. XAFS and bond-valence determination of mononuclear and polynuclear Pb(II) sorption products on aluminum oxides. *Geochim. Cosmochim. Acta* **61**, 2617–2637.

Bargar, J.R., Brown Jr., G.E., Parks, G.A., 1997b. Surface complexation of Pb(II) at oxide–water interfaces. II. XAFS and bond-valence determination of mononuclear Pb(II) sorption products and surface functional groups on iron oxides. *Geochim. Cosmochim. Acta* **61**, 2639–2652.

Chada, V.G.R., Hausner, D.B., Strongin, D.R., Rouff, A.A., Reeder, R.J., 2005. Divalent Cd and Pb uptake on calcite {1014} cleavage faces: an XPS and AFM study. *J. Colloid Interface Sci.* **288**, 350–360.

Cheng, L., Sturchio, N.C., Woicik, J.C., Kemner, K.M., Lyman, P.F., Bedzyk, M.J., 1998. High-resolution structural study of zinc ion incorporation at the calcite cleavage surface. *Surf. Sci.* **415**, L976–L982.

Dähn, R., Scheidegger, A.M., Manceau, A., Schlegel, M.L., Baeyens, B., Bradbury, M.H., Chateigner, D., 2003. Structural evidence for the sorption of Ni(II) atoms on the edges of montmorillonite clay minerals: a polarized X-ray absorption fine structure study. *Geochim. Cosmochim. Acta* **67**, 1–15.

Davis, J.A., Fuller, C.C., Cook, A.D., 1987. A model for trace metal sorption processes at the calcite surface: adsorption of $Cd^{2+}$ and subsequent solid solution formation. *Geochim. Cosmochim. Acta* **51**, 1477–1490.

Eick, M.J., Peak, J.D., Brady, P.V., Pesek, J.D., 1999. Kinetics of lead adsorption/desorption on goethite: residence time effect. *Soil Sci.* **164**, 28–39.

Elzinga, E.J., Reeder, R.J., 2002. X-ray absorption spectroscopy study of $Cu^{2+}$ and $Zn^{2+}$ adsorption complexes at the calcite surface: implications for site-specific metal incorporation preferences during calcite crystal growth. *Geochim. Cosmochim. Acta* **66**, 3943–3954.

Ford, R.G., Scheinost, A.C., Scheckel, K.G., Sparks, D.L., 1999. The link between clay mineral weathering and the stabilization of Ni surface precipitates. *Environ. Sci. Technol.* **33**, 3140–3144.

Ford, R.G., Kemner, K.M., Bertsch, P.M., 1999. Influence of sorbate-sorbent interactions on the crystallization kinetics of nickel- and lead-ferrihydrite coprecipitates. *Geochim. Cosmochim. Acta* **63**, 39–48.

Godelitsas, A., Astilleros, J.M., Hallam, K., Harissopoulos, S., Putnis, A., 2004. Interaction of calcium carbonates with lead in aqueous solutions. *Environ. Sci. Technol.* **37**, 3351–3360.

Hoffmann, U., Stipp, S.L.S., 2001. The behavior of $Ni^{2+}$ on calcite surfaces. *Geochim. Cosmochim. Acta* **65**, 4131–4139.

Lea, A.S., Amonette, J.E., Baer, D.R., Liang, Y., Colton, N.G., 2001. Microscopic effects of carbonate, manganese, and strontium ions on calcite dissolution. *Geochim. Cosmochim. Acta* **65**, 369–379.

Lee, Y.J., Elzinga, E.J, Reeder, R.J., 2005. Cu(II) Adsorption at the calcite-water interface in the presence of natural organic matter: kinetic studies and molecular-scale characterization. *Geochim. Cosmochim. Acta* **69**, 49–61.

Martin-Garin, A., Van Cappellen, P., Charlet, L., 2003. Aqueous cadmium uptake by calcite: a stirred flow-through reactor study. *Geochim. Cosmochim. Acta* **67**, 2763–2774.

Matocha, C.J., Elzinga, E.J., Sparks, D.L., 2001. Reactivity of Pb(II) at the Mn(III,IV) (oxyhydr)oxide–water interface. *Environ. Sci. Technol.* **35**, 2967–2972.

Meyer, H.J., 1984. The influence of impurities on the growth rate of calcite. *J. Crystal Growth* **66**, 639–646.

Möller, P., Sastri, C.S., 1974. Estimation of the number of surface layers of calcite involved in Ca-Ca45 isotopic exchange with solution. *Z. Physikalische Chemie* **89**, 80–87.

Paquette, J., Reeder, R.J., 1990. New type of compositional zoning in calcite: Insights into crystal growth mechanisms. *Geology* **18**, 1244–1247.

Paquette, J., Reeder, R.J., 1995. Relationship between surface structure, growth mechanism, and trace element incorporation in calcite. *Geochim. Cosmochim. Acta* **59**, 735–749.

Prieto, M., Cubillas, P., Fernández-González, A., 2003. Uptake of dissolved Cd by biogenic and abiogenic aragonite: A comparison with sorption to calcite. *Geochim. Cosmochim. Acta* **67**, 3859–3869.

Reeder, R.J., 1996. Interaction of divalent cobalt, zinc, cadmium, and barium with the calcite surface during layer growth. *Geochim. Cosmochim. Acta* **60**, 1543–1552.

Reeder, R.J., Lamble, G.M., Northrup, P.A., 1999. XAFS study of the coordination and local relaxation around $Co^{2+}$, $Zn^{2+}$, $Pb^{2+}$, and $Ba^{2+}$ trace elements in calcite. *Am. Mineral* **84**, 1049–1060.

Ressler, T., 1997. WinXAS: A new software package not only for the analysis of energy-dispersive XAS data. *J. Physique IV* **7**, C2–269.

Rouff, A.A., Reeder, R.J., Fisher, N.S., 2002. Pb(II) sorption with calcite: a radiotracer study. *Aquatic Geochem.* **8**, 203–228.

Rouff, A.A., Elzinga, E.J., Reeder, R.J., Fisher, N.S., 2004. X-ray absorption spectroscopic evidence for the formation of Pb(II) inner-sphere adsorption complexes and precipitates at the calcite-water interface. *Environ. Sci. Technol.* **38**, 1700–1707.

Rouff, A.A., Elzinga, E.J., Reeder, R.J., Fisher, N.S., 2005. The influence of pH on the kinetics, reversibility and mechanisms of Pb(II) sorption at the calcite-water interface. *Geochim. Cosmochim. Acta* **69**, 5173–5186.

Rouff, A.A., Elzinga, E.J., Reeder, R.J., Fisher, N.S., 2006. The effect of aging and pH on Pb(II) sorption processes at the calcite-water interface. *Environ. Sci. Technol.* **40**, 1792–1798.

Scheckel, K.G., Scheinost, A.C., Ford, R.G., Sparks, D.L., 2000. Stability of layered Ni hydroxide surface precipitates—a dissolution kinetics study. *Geochim. Cosmochim. Acta* **64**, 2727–2735.

Scheckel, K.G., Impellitteri, C.A., Ryan, J.A., 2004. Lead sorption on ruthenium oxide: a macroscopic and spectroscopic study. *Environ. Sci. Technol.* **38**, 2836–2842.

Schosseler, P.M., Wehrli, B., Schweiger, A., 1999. Uptake of $Cu^{2+}$ by the calcium carbonates vaterite and calcite as studied by continuous wave (CW) and pulse electron paramagnetic resonance. *Geochim. Cosmochim. Acta* **63**, 1955–1967.

Stipp, S.L., Hochella, M.F., Parks, G.A., Leckie, J.O., 1992. $Cd^{2+}$ uptake by calcite, solid-state diffusion, and the formation of solid-solution: Interface processes observed with near-surface sensitive techniques (XPS, LEED, and AES). *Geochim. Cosmochim. Acta* **56**, 1941–1954.

Stipp, S.L.S., 1994. Understanding interface processes and their role in the mobility of contaminants in the geosphere: The use of surface sensitive techniques. *Eclogae Geologicae Helvetiae* **87**, 335–355.

Stipp, S.L.S., 1998. Surface analytical techniques applied to calcite: evidence of solid- state diffusion and implications for isotope methods. *Palaeogeogr. Palaeoclimatol. Palaeoecol.* **140**, 441–457.

Strawn, D.G., Scheidegger, A.M., Sparks, D.L., 1998. Kinetics and mechanisms of Pb(II) sorption and desorption at the aluminum oxide water interface. *Environ. Sci. Technol.* **32**, 2596–2601.

Sturchio, N.C., Chiarello, R.P., Cheng, L.W., Lyman, P.F., Bedzyk, M.J., Qian, Y.L., You, H.D., Yee, D., Geissbuhler, P., Sorensen, L.B., Liang, Y., Baer, D.R., 1997. Lead adsorption at the calcite–water interface: synchrotron X-ray standing wave and X-ray reflectivity studies. *Geochim. Cosmochim. Acta* **61**, 251–263.

Temmam, M., Paquette, J., Vali, H., 2000. Mn and Zn incorporation into calcite as a function of chloride aqueous concentration. *Geochim. Cosmochim. Acta* **64**, 2417–2430.

Tesoriero, A.J., Pankow, J.F., 1996. Solid solution partitioning of $Sr^{2+}$, $Ba^{2+}$ and $Cd^{2+}$ to calcite. *Geochim. Cosmochim. Acta* **60**, 1053–1063.

Trivedi, P., Dyer, J.A., Sparks, D.L., 2003. Lead sorption onto ferrihydrite. 1. A macroscopic and spectroscopic assessment. *Environ. Sci. Technol.* **37**, 908–914.

Van der Weijden, R.D., Van der Weijden, C.H., Comans, R.N.J., 1994. Sorption and sorption reversibility of cadmium on calcite under simulated riverine, estuarine and marine conditions. *Marine Chem.* **47**, 65–79.

Van der Weijden, R.D., Meima, J., Comans, R.N.J., 1997a. Sorption and sorption reversibility of cadmium on calcite in the presence of phosphate and sulfate. *Marine Chem.* **57**, 119–132.

Van der Weijden, R.D., Van der Heijden, A.E., Witkamp, G.J., Van Rosmalen, G.M., 1997b. The influence of total calcium and total carbonate on the growth rate of calcite. *J. Crystal Growth* **171**, 190–196.

Zachara, J.M., Kittrick, J.A., Harsh, J.B., 1988. The mechanism of $Zn^{2+}$ adsorption on calcite. *Geochim Cosmochim. Acta* **52**, 2281–2291.

Zachara, J.M., Kittrick, J.A., Dake, L.S., Harsh, J.B., 1989. Solubility and surface spectroscopy of zinc precipitates on calcite. *Geochim. Cosmochim. Acta* **53**, 9–19.

Zachara, J.M., Cowan, C.E., Resch, C.T., 1991. Sorption of divalent metals on calcite. *Geochim. Cosmochim. Acta* **55**, 1549–1562.